EVIDENCE FROM THE MOTIONS OF GALAXIES FOR A LARGE-SCALE, LARGE-AMPLITUDE FLOW TOWARD THE GREAT ATTRACTOR

DAVID BURSTEIN
Department of Physics and Astronomy, Arizona State University

S. M. FABER
Lick Observatory, University of California, Santa Cruz

AND

ALAN DRESSLER
The Observatories of the Carnegie Institution of Washington

ABSTRACT

We have combined the available distances of galaxies to produce a unified view of galaxy motions within the so-called great attractor (GA) region. The current data base includes 253 galaxies that lie within 40° of the nominal GA center, 3.5 times the number of galaxies in the original Lynden-Bell et al. survey. The motions of galaxies in all data sets support the basic picture of a high-velocity flow as described by Lynden-Bell et al. and Faber and Burstein. Within 40° of the center of this region, the flow velocity rises outward from the Local Group, reaching a maximum of ~ 1000 km s^{-1} at a distance of ~ 2000 km s^{-1}, then decreasing to near zero at a distance of 4500 km s^{-1}. This latter distance is close to the centroid of the radial velocity distribution observed for galaxies in this region by Dressler, suggesting that this region can plausibly be equated with the center of mass of the GA. Although the present observations go deeper than the original Lynden-Bell et al. data, an unambiguous signature of infall by galaxies on the backside of the GA has not yet been obtained, possibly because of Malmquist-bias selection effects.

A previous model of the Centaurus clusters as two closely interacting clusters is examined in detail using distances to 47 galaxies previously identified as cluster members. Although the existence of two separate clusters is blurred in the present sample, the majority of galaxies are clearly on the near side of the GA center, falling into the GA.

Checks are made for systematic errors in the motions of ellipticals that are correlated with cluster richness, structural parameters of the galaxies, or errors in Galactic absorption. Two small effects are found, but neither has a significant effect on the observed large-scale motions. Other evidence strongly supporting the current distance indicators is reviewed, and arguments are presented in favor of the cosmic background radiation defining the correct velocity rest frame. The basic conclusion of this study is therefore to affirm the fundamental correctness of the present body of measured galaxy motions.

Subject headings: galaxies: clustering — galaxies: redshifts

I. INTRODUCTION

Our recent study of galaxy streaming motions (Burstein et al. 1986; Dressler et al. 1987; Lynden-Bell et al. 1988, hereafter 7S) has claimed to detect a large-scale, coherent motion of galaxies toward a mass concentration in the constellation Centaurus. This concentration, dubbed the "great attractor"[1]

(GA) by Dressler (1988), has its center at an estimated distance of ~ 4500 km s^{-1} (see Faber and Burstein 1989). A subsequent redshift survey by Dressler (1988), extending earlier work by Chincarini and Rood (1979), Hopp and Materne (1985), and Melnick and Moles (1987), found a large overdensity of galaxies having a centroid redshift near 4000 km s^{-1}, spanning

---

[1] A clarification of terminology is warranted because we find that, even among ourselves, we have been using the term "great attractor" to mean different things. Burstein and Faber used the term to refer to the central core of the large, overdense region found by Dressler in his radial velocity survey. This core is roughly 1000 km s^{-1} in radius, centered on ~ 4500 km s^{-1} and is equivalent to the core region of the revised spherical flow model by Faber and Burstein (1989). The core subtends roughly 30° diameter on the sky and corresponds to the high-density region visible in Lahav's picture in Lynden-Bell et al. With this definition, the Centaurus clusters are barely in the foreground of the GA, while the Hydra and Antlia clusters are off to one side of it.

Dressler has used the term "great attractor" to mean the entire overdense region within the sphere centered on 4500 km s^{-1} and with radius out to the Local Group; hence, all matter that would generate the GA flow velocity at our location in the spherically symmetric model is included. In this picture, the Centaurus clusters, Hydra, and Antlia are all part of the great attractor.

Since Dressler introduced the term, we will henceforth adhere to his usage, reserving the term "GA center" to refer to the core regions. The idea of a smooth, homogeneous core is of course an idealization. Future studies may

show the central regions to be so lumpy as to render the word "core" meaningless and even misleading. If so, more appropriate terminology will have to be developed. Sometimes, for shorthand we speak of a direction or flow "toward the GA." By this we always mean the direction toward the center of the GA.

Two other terms that have been used in recent papers also merit clarification. The "Centaurus concentration," as defined by Lynden-Bell and Lahav, refers to the dense concentration of galaxies on the sky lying to the Galactic north ($l = 310°$, $b = 38°$) of the nominal Centaurus clusters. The terms "Centaurus Supercluster" or "Hydra-Centaurus Supercluster" have been used interchangeably by many authors (e.g., Chincarini and Rood 1979; Fairall and Winkler 1984; Hopp and Materne 1985; Lucey, Currie, and Dickens 1986) to denote the enhanced density of galaxies in the region bounded by $260° < l < 320°$, $10° < b < 40°$. In our present terminology, the name great attractor encompasses all these terms, because they each can be viewed as being part of this larger entity (which also includes Antlia and Pavo-Indus).

the range in radial velocity from 2000 to 5500 km s^{-1}, and spread out over nearly a steradian on the sky.

In an accompanying paper, Dressler and Faber (1990, hereafter DF) present preliminary results from a new diameter-limited survey of E and S0 galaxies toward the GA, selected from the redshift survey of Dressler (1988). Measurements of all galaxies agree well with the data from 7S and show a coherent, rising flow away from the Local Group, with a maximum amplitude of ~ 1000 km s^{-1} at roughly 2000 km s^{-1} in distance. The flow declines beyond that point, approaching zero in the neighborhood of 4500 km s^{-1}, consistent with the prediction of the revised spherically symmetric flow model of Faber and Burstein (1989).

In addition to the surveys of 7S and DF, four other studies have produced distance estimates to galaxies in the direction of the GA: the survey of field spirals by Aaronson et al. (1982a, b, collectively referred to as AHM), the field spiral survey by de Vaucouleurs and Peters (1984, hereafter dVP), recent measurements of field and cluster spirals by Aaronson et al. (1986, hereafter A86; 1989, hereafter A89), and new cluster E/S0 galaxies by Lucey and Carter (1988, hereafter LC). The casual reader of these papers might be rightfully confused. The two former surveys did not recognize the existence of any flow toward the GA. The latter two papers disagree with each other in detail on the distances of certain clusters. Moreover, these papers leave the reader with the impression that a generally smaller, even zero, net flow exists in the direction of the GA, is directed at known clusters, and exists over a smaller range in solid angle as compared to the picture developed by 7S.

Although several surveys of distances to galaxies in the GA region are currently in progress, we feel that sufficient data now exist from all sources to produce a unified, significantly updated picture of galaxy motions in this direction. The major result is a strong reinforcement of the original picture of the GA advocated by 7S and reasonable agreement (over the volume so far surveyed) with the revised spherically symmetric infall model of Faber and Burstein (1989) (see discussion in Burstein 1990b for a more detailed comparison of these data to the GA model).

II. THE MERGED DATA SAMPLE

The area studied has a radius of 60° on the sky centered on the direction $l = 309°$, $b = +18°$, the revised centroid of the Faber-Burstein model. The merged data sets are summarized in Table 1. Together they contain 170 elliptical galaxies and 83 spiral galaxies within 40° of the GA center, an increase of 3.5

times over the original 69 galaxies of 7S within the same region. Even so, the sample is still somewhat incomplete, being overrepresented by galaxies in the environs of clusters. The distribution of galaxies with measured distances on the sky and lying within 60° of the GA center (413 galaxies in all) is shown in Figure 1, with the major groups labeled.

The AHM data can be objectively divided into two subsets: those with consistent, reliable diameters and axial ratios, and those without (Faber and Burstein 1989). The estimated observational errors in the Tully-Fisher relation for the former, well-observed subset are $\lesssim 0.35$ mag (AHM "good"), while those for the less well observed set (AHM "fair") are 0.49 mag. (Burstein and Raychaudhury 1989 have suggested that the intrinsic ~ 0.7 mag scatter in the Tully-Fisher relation, claimed by Kraan-Korteweg, Cameron, and Tammann 1988, is due to larger observational errors in the blue magnitudes for that sample.) Error estimates for both subsets of the AHM data are less than those estimated for the dVP sample (0.55 mag), and the AHM data are used here in preference to the dVP data when they are available. In addition, use of the dVP data is limited to galaxies with Local Group velocities less than 1400 km s^{-1} to avoid complications with an apparent distant-dependent scale error (see Faber and Burstein 1989).

Measurements for E/S0 galaxies from all sources (7S, LC, and DF) have been averaged with equal weight (estimated error of 21% in distance). This procedure has maximized the total sample by combining partial data from different observers. Galactic extinction corrections for spirals are as quoted by the original authors, and corrections for the E/S0 galaxies are taken from Burstein and Heiles (1978, 1982) with modifications as described in the Appendix.

To reduce the effect of Malmquist bias errors (see Lynden-Bell et al. 1988), we have grouped galaxies into clusters using our previous precepts (Davies et al. 1987; Faber et al. 1989). Since one of the aims of this paper is to compare motions of spirals and ellipticals, the groupings for these types have been determined separately. With the exception of the two Centaurus clusters (here named Cen 30 and Cen 45 after the radial velocity convention adopted by Lucey, Currie, and Dickens 1986; see § V), authors' group and field memberships have been taken from the original sources (see Table 1). Groupings have also been provided for the Dressler-Faber E/S0 galaxies, which is a change from the accompanying paper (Dressler and Faber 1990, hereafter DF). Spirals with reliable observations not classified as cluster members by A89 have been retained as field galaxies (a total of 14 galaxies). The confused situation

TABLE 1

DATA SOURCES FOR GALAXIES WITH MEASURED DISTANCES IN THE GREAT ATTRACTOR REGION
($\leq 40°$ OF $l = 309°$, $b = 18°$)

Source	Galaxy Type and Region	Number[a]
Aaronson et al. 1982, 1989	Field spirals ("good" and "fair")[b]	14
de Vaucouleurs and Peters 1984	Field spirals (blue TF data only) with Local Group velocities ≤ 1400 km s^{-1}	10
Lynden-Bell et al. 1988, Faber et al. 1989	Mag-limited E survey	69
Aaronson et al. 1986, 1989	Spirals in and near seven clusters	58
Lucey and Carter 1988	E and S0 galaxies in four clusters	30
Dressler and Faber 1989	Deeper diameter-limited E/S0 survey	110
Total Number of Galaxies		253[c]

[a] The number of galaxies in each survey.

[b] See text and Faber and Burstein 1989 for a description of "good" and "fair" subsets of the AHM data.

[c] This total reflects the number of galaxies used here. The merging of the three elliptical surveys creates a merged list with fewer galaxies than would be obtained by summing the individual sources; see text.
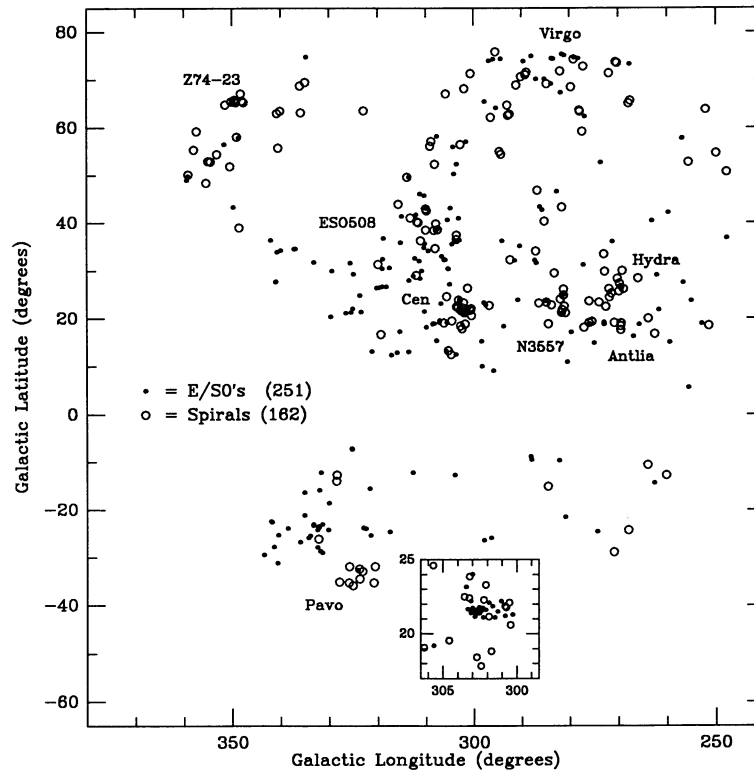
FIG. 1.—The distribution on the sky, in Galactic coordinates, of 413 galaxies with measured distances that lie within a 60° radius of the nominal center of the great attractor region at $l = 309°$, $b = 318°$. The positions of 251 ellipticals are marked with small closed circles, those for 162 spirals with large open circles. The prominent groups and clusters in this region are identified by their most common names. The small insert at the bottom of the figure is an enlargement of the region in the vicinity of Centaurus.

with Centaurus cluster memberships is discussed separately in § V.

Distances (R) are calculated as in Lynden-Bell et al. and expressed in units of km s^{-1}, with the distance of the Coma Cluster (7380 km s^{-1}) used as zero point (note the small difference from the distance assumed by Lynden-Bell et al. and DF). With this distance, the Coma Cluster is inferred to have a peculiar velocity of -180 km s^{-1} in the cosmic background radiation (CBR) reference frame. The distance of an individual galaxy is defined as R_{IND}; cluster galaxies can also be assigned the median cluster distance, R_{CL} (a difference in treatment from DF). R_{IND} is used mainly for field and singly observed galaxies in clusters ("singles"), while R_{CL} is used primarily for galaxies in a given cluster with two or more measured galaxies. Exceptions to this convention will be noted. Radial velocities are measured in the CBR reference frame, V_{CBR}, and are the measured velocity for field galaxies, and the cluster velocity for cluster galaxies (including singly-measured galaxies), except where noted (e.g., for Fig. 5).

III. PECULIAR MOTIONS

DF have demonstrated that their new E/S0 data agree well with the original 7S motions. We show here that all other available data also agree and, in particular, that spirals and E/S0 galaxies agree well with one another. The evidence is shown in Figures 2 and 3, which plot peculiar velocity $(V_{CBR} - R)$ versus distance in both cones and annular rings centered on the direction $l = 309°$, $b = 18°$. The distance to the Centaurus clusters is handled in two different ways (see

caption to Fig. 2), and the two columns of graphs illustrate data with and without Malmquist bias correction (see § IV).

Elliptical galaxy and spiral galaxy peculiar motions agree well at all distances from the GA, and clusters agree well with the elliptical "single" and spiral field galaxies. Figure 2 shows the motions of galaxies with measured distances located that lie within 20° of the GA center. Collectively, the data show the same pattern of motions described by DF: a gradual rise in velocity away from the Local Group to a maximum of ~1000 km s^{-1} at ~2000 km s^{-1}, declining beyond that point to near zero around 4500 km s^{-1}. This rise and fall are significant for four reasons:

1. The high positive velocities are not likely to be caused by Galactic absorption errors. A uniform absorption error would cause an error in peculiar motion that is proportional to distance and would thus yield a straight rising line of constant slope, not a rise and fall as seen here (see also discussion in the Appendix and in DF).

2. A zero-point error in the distance indicators would also cause an error in peculiar motion that is proportional to distance. Hence, if zero-point deviations are important, they must be confined to the localized region 1000–3500 km s^{-1} and must be largest in the central zones. Furthermore, the deviations for spirals and ellipticals must be virtually the same. In other words, such zero-point errors would have to precisely mimic all the observed motions associated with a large region of infall.

3. The continued decline in velocity beyond 3000 km s^{-1} is consistent with the 7S model of a major mass concentration
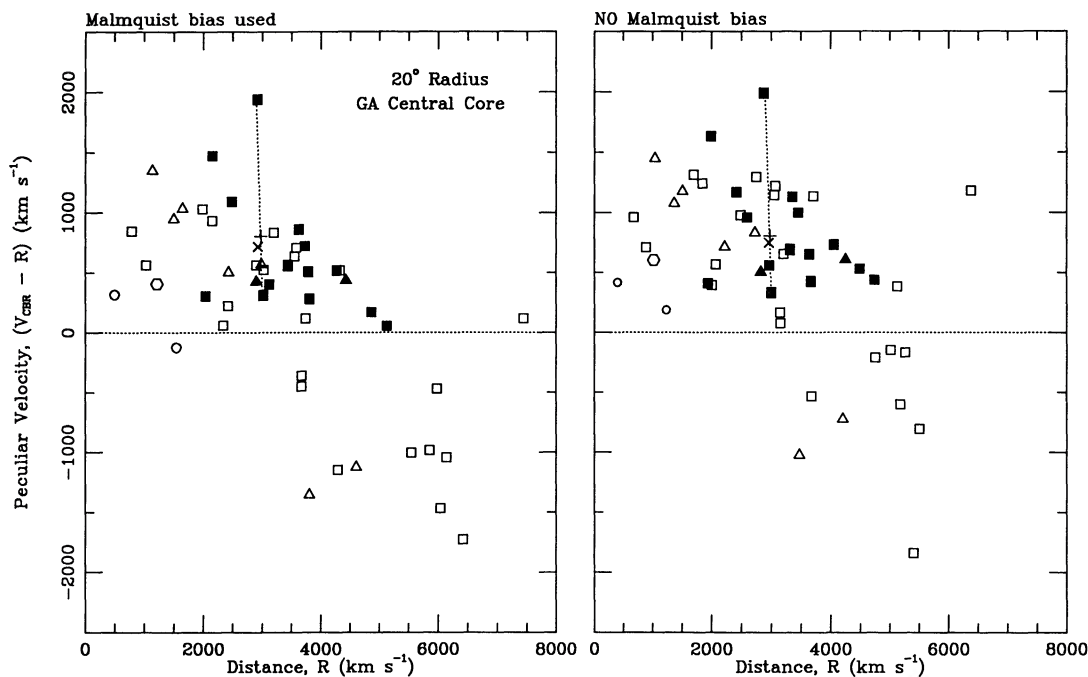
FIG. 2.—Peculiar motions ($V_{CBR} - R$) km s^{-1}, plotted vs. distance, R km s^{-1}, for galaxies lying within a cone of 20° width, centered on the GA center. R_{IND} is used for field galaxies, R_{CL} for cluster galaxies. The left graph uses distances corrected for Malmquist bias due to a homogeneous galaxy distribution ("with bias correction"; see Fig. 4a). The right graph uses raw distances with no Malmquist bias correction ("without bias correction"). Symbols for both this figure and Fig. 3 are: *open squares*—"single" elliptical galaxies; *closed squares*—ellipticals in clusters; *open triangles*—field spiral galaxies from the Aaronson *et al.* "good" sample; *closed triangles*—Aaronson *et al.* spiral-defined clusters; *open hexagons*—field spiral galaxies from the Aaronson *et al.* "fair" sample; *small open circles*—field spiral galaxies from the sample of de Vaucouleurs and Peters. The net motions of the Cen 30 and Cen 45 clusters are represented in two different ways: the motion of all 47 galaxies (noted by an X) and the motion of the Cen 30 and Cen 45 ellipticals, calculated for a mass ratio of 3:1 for Cen 30:Cen 45 (see Table 2). The two clusters treated as separate entities are connected by a dotted line. This figure is the most complete view of motions toward the center of the GA afforded by the present data.

centered *beyond* 3000 km s^{-1} and pulling foreground galaxies toward it. As the weightiest object in the region, the center of this mass should move more slowly than the foreground, and this is consistent with the observed velocity turnover. The zero crossing near 4500 km s^{-1} is also consistent with Dressler's (1988) measured velocity centroid near 4000 km s^{-1}.

4. A velocity decline contradicts the suggestion of Scarmella *et al.* (1989) that an even more massive concentration of clusters near 14,000 km s^{-1} is causing much of the GA flow. That model would predict a continuing rise in velocity at large distances, as the neighborhood of the distant mass concentration is approached.

Figure 3 shows the motions of galaxies as a function of angular distance from the center of the GA. The curves plotted in this figure are the predicted motions of the revised spherically symmetric infall model of Faber and Burstein (1989), plotted here to represent a simple model of these motions. This model inserts a core radius into the original power-law model of Lynden-Bell *et al.* and was optimized by fitting to the original 69 7S galaxies plus a handful of AHM field spirals. A core radius was added because the average peculiar velocity beyond 3000 km s^{-1} seemed to fall, based on the few galaxies (mainly Es) then available. This hint of a decline is confirmed by the new data, as shown in Figure 2. Moreover, the peculiar motions appear to die away smoothly in the zones 10° and greater in angle away from the infall center (Figs. 3b–3f), more or less as predicted by the spherically symmetric model. However, the spherically symmetric model does not fit the motions well in the very center of the GA (Fig. 3a), where it predicts infall velocities that are higher than observed. This

suggests that the peak mass densities in the center of the GA are not as high as predicted by the model. The elliptical galaxies with large positive motions in Figure 3c are located in the Pavo-Indus region, which is suspected to be another region with large internal motions (Faber and Burstein 1989).

We conclude that the spherical model is a reasonable description of the flow over the near side of the GA at radii greater than 10°. Rough spherical symmetry would imply a density distribution and flow on the *backside* that are similar to those on the near side. Backside infall should show up as a negative-velocity tail of galaxies beyond the zero-crossing point. There is a scattering of objects in Figure 2 that might qualify as this negative velocity tail. This brings us to an important question: Has backside infall been detected?

IV. BACKSIDE INFALL

The backside of the GA cannot be discussed without raising the issue of Malmquist bias. Malmquist bias is caused by coupling between the errors of measurement and the space distribution of galaxies, which can result in spurious trends in observed peculiar motions versus distance. Our group has collectively termed these errors "Malmquist bias," although the form of the error resembles classical Malmquist bias only for smooth, power-law variations in space density (see Lynden-Bell *et al.* 1988). For an accurate estimate of Malmquist bias, independent detailed knowledge of the space distribution of the sample is required.

Unfortunately it is impossible to infer the true space distribution of galaxies easily from Figures 2 and 3. For the E/S0 galaxies, sample incompleteness is rapidly increasing between
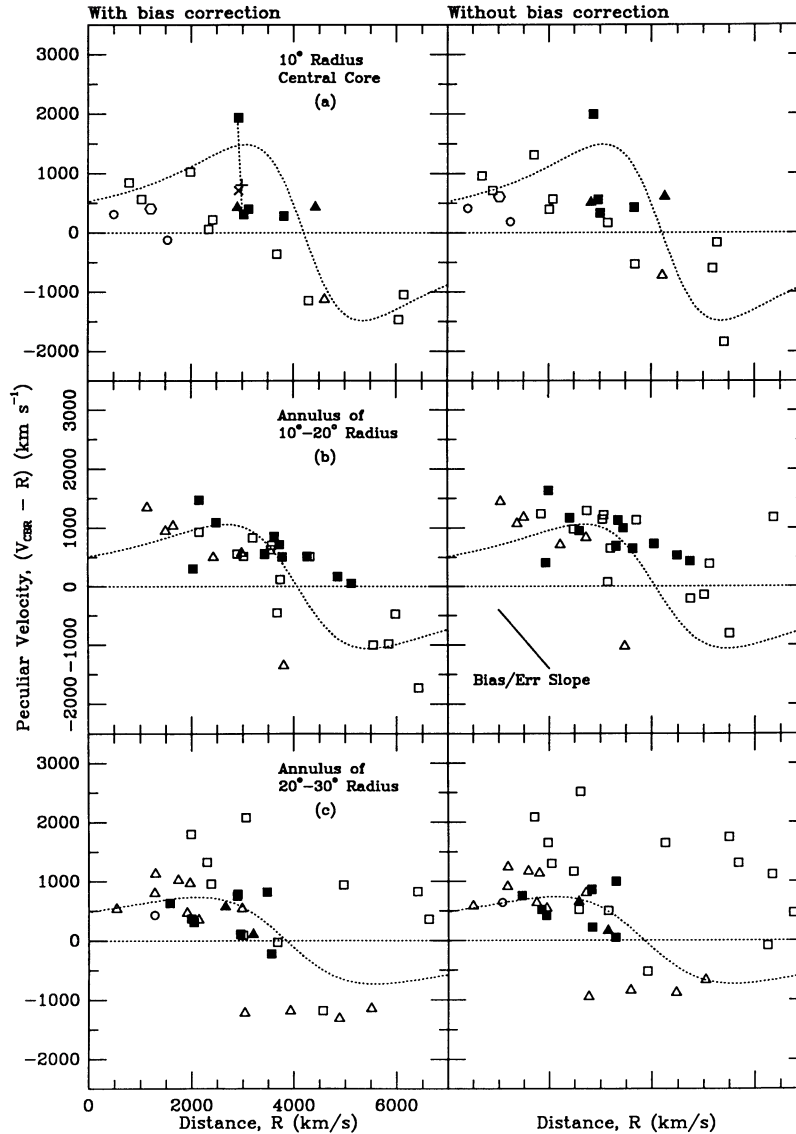
FIG. 3.—Peculiar velocity vs. distance as a function of angular distance from the center of the GA. Symbols, definition of data, and meaning of the two graphs for each set of figures are the same as in Fig. 2. (a) The peculiar motions of galaxies within a cone of 10° width, centered on $l = 309°$, $b = 18°$. (b)–(f) The peculiar motions of galaxies in annuli of 10° width, graduated outward in intervals of 10° (i.e., Fig. 2b has 10°–20°, Fig. 2c 20°–30°, etc.). The curved dotted line in each graph represents the predicted peculiar velocity of the GA model velocity field of Faber and Burstein (1989) for the center angular distance of the annulus or cone from the center of the GA.

3000 and 6000 km s^{-1}, and the overall falloff in galaxies beyond 4000 km s^{-1} is due mainly to this. From comparing to the rest of the 7S sample *outside* the GA, an extra break, or "cliff," in the space distribution of E/S0 galaxies near 5000 km s^{-1} seems to be a possibility. We defer further discussion and modeling of this break to a future paper on the completed DF survey. One should nonetheless keep in mind that there could be a strong dropoff in the space distribution of early-type galaxies toward the GA beyond 5000 km s^{-1}.

Less is known about the space distribution of spirals. There may also be a break in their density distribution, but preliminary evidence (from radial velocities) suggests that it is less severe. This difference in spatial distribution between early- and late-type galaxies is consistent with the morphological

density relation for galaxies found in this and other areas of the sky (e.g., Dressler 1980).

Three possible models for Malmquist bias toward the GA are sketched schematically in Figure 4, corresponding to different space density profiles through the GA. The figure plots the run of peculiar motion versus raw distance expected from bias errors alone (i.e., no real motions of galaxies are implied) and should be compared to the right halves of Figures 2 and 3, which plot raw motions uncorrected for bias. The uniform-density case is shown in panel (a) by a dashed line of constant slope (Lynden-Bell et al., eq. [2.11]). This slope, and hence the bias, is proportional to (distance error)^2. A cluster of galaxies at a single distance from us is shown in Figure 4b. Galaxies are scattered into the foregound and background of the cluster by
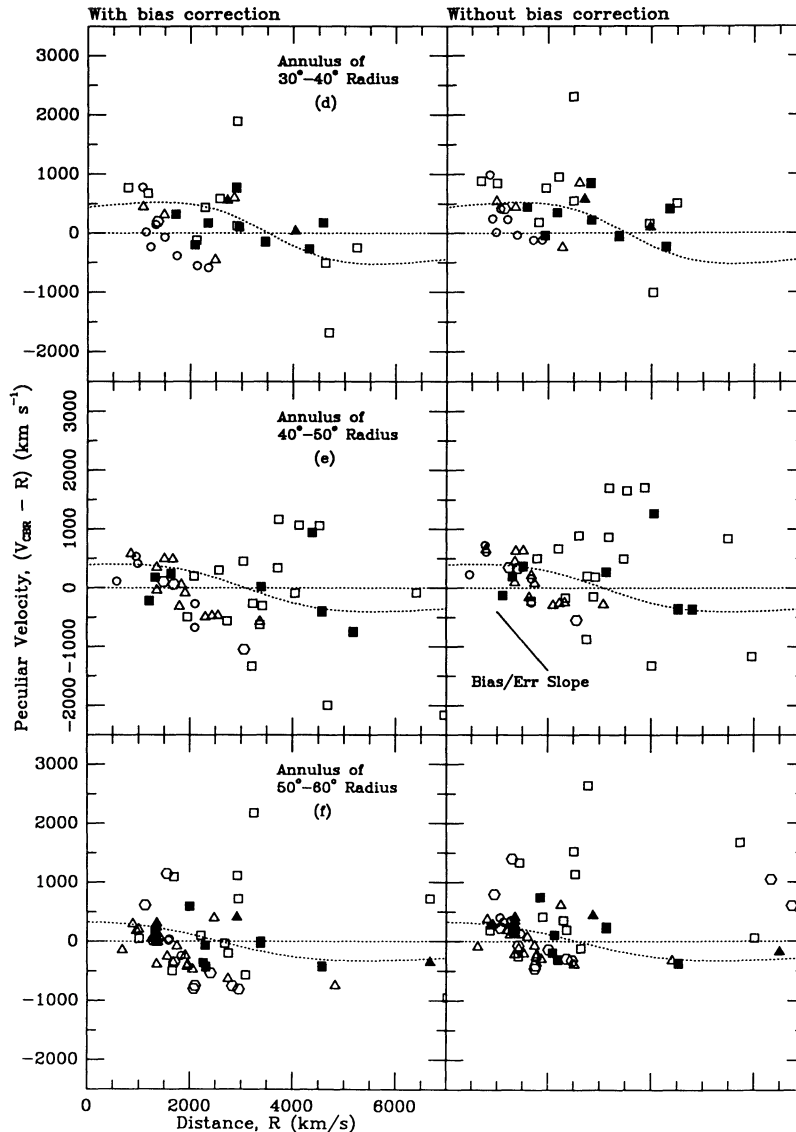
FIG. 3—Continued

errors. The resultant locus follows an error slope of -1, and the total length of the locus is proportional to the size of the distance error at the cluster (Faber and Burstein 1989). If enough galaxies are sampled, the true distance of the cluster is essentially given by the median of the observed distances.

The third case, in Figure 4c, may be the one that is most relevant to the center of the GA, at least for the early-type galaxy component. This panel shows schematically the bias for a uniform space distribution of galaxies with a sharp outer boundary, taken here to be at 5000 km s^{-1}. Well inside the boundary, the bias behaves as for uniform density. In the vicinity of the boundary, the bias changes sign and has slope of -1 beyond it. No galaxies actually exist beyond the boundary but are scattered there by errors. As for a single cluster, the length of the negative tail is proportional to the size of the distance error at the boundary. In all three panels, the amplitude of the bias shown is intended to match fairly closely the actual errors of measurement in the present sample, averaged over galaxy types.

The sizes and signs of bias in the three cases are clearly

different, illustrating the fact that the raw observed velocity field depends critically on the space density along the line of sight when observational errors are comparable to or larger than true peculiar velocities. For now, we illustrate the possible magnitude of Malmquist effects by comparing just two elementary cases in Figures 2 and 3—raw motions uncorrected for any Malmquist effect, and motions corrected for uniform density. The actual errors of measurement have been used to correct each point individually. As a result, clusters move less between the two diagrams than field galaxies, providing an additional constraint on the range of possible motions.

Figures 2 and 3 show that the uniform density correction has relatively little effect on the gross topology of the curves: Although the maximum velocity is slightly smaller in the corrected case, the rise, fall, and zero crossing near 4500 km s^{-1} remain substantially the same. To the extent that the space distribution of galaxies is fairly uniform out to 3000 km s^{-1}, the strong, positive motions seen over that range *cannot* be caused by Malmquist errors—the observed perturbations are far too large.
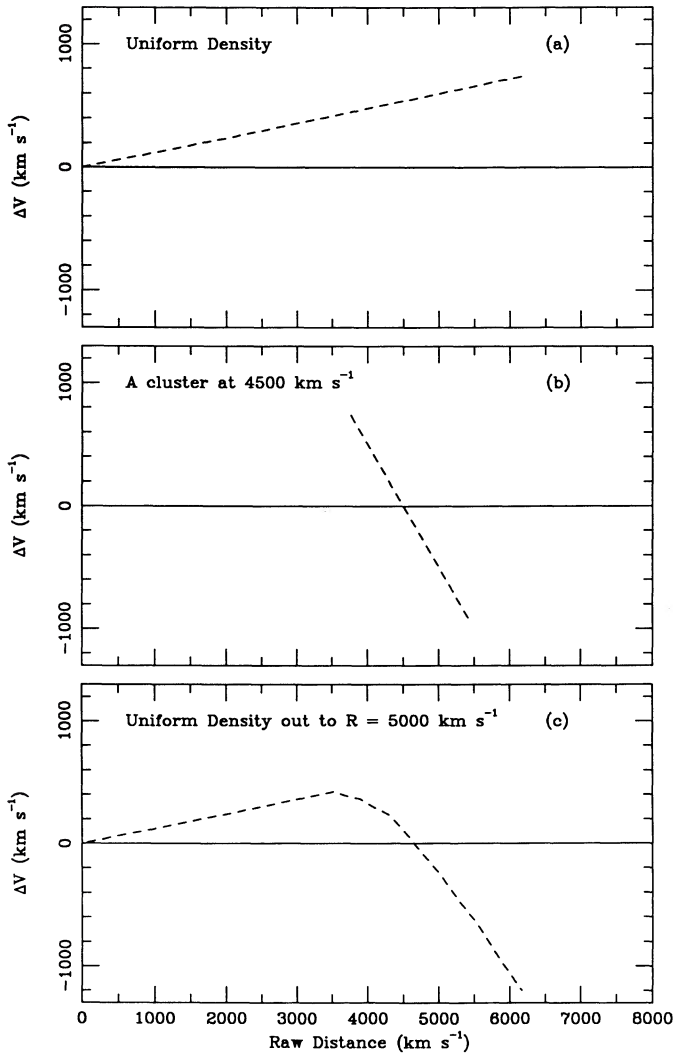
FIG. 4.—Schematic examples of Malmquist-type bias errors in peculiar motions as a function of distance that can result from three possible density distributions along the line of sight to the great attractor. The size of error corresponds roughly to the observational errors in the real data. (a) If the galaxies are distributed uniformly along the line of sight, Malmquist-bias will have peculiar motions that increase in proportion to distance. (b) If the galaxies are all situated near a single distance (as they would be if all in the same cluster), then Malmquist-bias errors yield peculiar velocity errors that correlate with a slope of -1, centered at that distance. (c) If the galaxies are distributed uniformly up to a distance of 5000 km s^{-1}, at which there is a sharp cutoff, then the Malmquist-bias errors would produce peculiar velocity errors that are a mixture of those illustrated in (a) and (b).

On the other hand, the negative-velocity tail could be strongly affected by Malmquist bias. As Figure 4c shows, the very existence of such a tail could be illusory, caused by scattering errors at the boundary of a density discontinuity. Since the observed tail is comprised largely of E/S0 galaxies, the role of a density discontinuity may be particularly important. Conclusions on the amount and extent of backside infall will therefore have to await a statistically valid sample that penetrates well beyond the central region, preferably of spirals which may have a more uniform space distribution.

To summarize, the totality of available motions toward the GA agrees well with the picture originally outlined by Lynden-Bell et al. The velocity perturbation is extensive, subtending more than 60° in radius on the sky, and declines with angular

distance away from the center of the GA roughly as described by the spherical model of Faber and Burstein (1989). Peculiar motions of field and cluster galaxies, E/S0 galaxies and spirals, are all the same. The turnover in velocity beyond ~ 2000 km s^{-1} virtually eliminates the most obvious sources of systematic error. Even so, infall from the backside cannot yet be unambiguously identified from the present data set.

This analysis differs in certain important respects from conclusions reached by the original sources of these data. These differences turn out to hinge crucially on the role and significance of the motion of the Centaurus clusters, to which we now turn.

V. THE CENTAURUS CLUSTERS

The Centaurus clusters (termed Cen 30 and Cen 45 by Lucey, Currie, and Dickens 1986) are the most prominent density concentrations on the near flank of the GA center. Although they have played an important historical role in developing the GA picture, the large amount of additional data now available makes our understanding of the GA region much less dependent on these two clusters. Nonetheless, their mean flow relative to the GA is still of interest and, with 47 measured galaxies, they provide an interesting test of our ability to disentangle the structure of a complex region (see Lucey et al. 1990).

Previous measurements of the motions of the Centaurus clusters are summarized in Table 2A. The original study by Lynden-Bell et al. found very high peculiar motions for both components: Cen 30 = 1110 km s^{-1} and Cen 45 = 1663 km s^{-1} (no Malmquist corrections), based on five and four ellipticals, respectively. Using spirals, Aaronson et al. (A89) measured smaller motions of only 606 and 504 km s^{-1}. Recent measurements using E/S0 galaxies by Lucey and Carter found a large motion for Cen 45 of 2242 km s^{-1} based on seven galaxies but a very small velocity for Cen 30 of only 244 km

TABLE 2A

PECULIAR MOTIONS OF THE CENTAURUS CLUSTERS

	Cen 30[a]		Cen 45[a]	
SOURCE	Peculiar Velocity (km s^{-1})	N	Peculiar Velocity (km s^{-1})	N
Lynden-Bell et al. 1988 (Es)	1110 ± 208	5	1663 ± 334	4
Aaronson et al. 1989 (spirals)	489 ± 253	10	588 ± 453	6
Lucey and Carter 1988 (E/S0's)	244 ± 335	15	2242 ± 285	7
This paper[b]:				
Spirals	504 ± 180	10	606 ± 456	6
E/S0's	310 ± 150	22	1937 ± 220	9

[a] Local Group radial velocities assumed are 2809 km s^{-1} for Cen 30 and 4313 km s^{-1} for Cen 45.

[b] Raw values; no Malmquist correction applied.

TABLE 2B

MEDIAN VALUES OF RADIAL VELOCITY AND DISTANCE

Source	CBR Radial Velocity (km s^{-1})	Distance (km s^{-1})	Peculiar Velocity (km s^{-1})
This paper (16 spirals, 31 E/S0's)[a]	3790	2984	806

NOTE.—If Cen 30 is 3 times the mass of Cen 45, then the center of mass peculiar velocity of their ellipticals is 716 km s^{-1}.

[a] All galaxies treated as one cluster; see text for details.

s^{-1} from 15 galaxies. This small motion led LC to suggest Cen 30 as the center of mass producing the acceleration for the whole GA region, Cen 45 included. Such an interpretation is clearly at variance with the picture of Lynden-Bell et al., who stressed that both clusters are in the foreground of a more massive, more extended, and more distant mass concentration. As is shown below, the disagreements among quoted peculiar motions for these two clusters are primarily due to random samplings of galaxies in a complicated region, in which distance and radial velocity are poorly correlated.

In Figures 2 and 3, we plot the motions of the Centaurus clusters using the median distances listed near in Table 2B, following the radial velocity selection criterion for the two clusters advocated by Lucey et al. The essential ambiguity of dividing the clusters this way is illustrated in Figures 5 and 6. The individual motions of the 47 galaxies are plotted in Figure 5 (using R_{IND}, V_{CBR}, and no Malmquist bias; see figure caption). The histogram distribution of distances and CBR radial velocities for the 47 galaxies are plotted in Figures 6a and 6b.

Figure 5 shows that both spirals and E/S0 galaxies populate similar ranges in distance, independent of whether they are assigned to Cen 30 or Cen 45. The higher motions of the Cen 45 galaxies are simply the necessary consequence of their having been assigned to the Cen 45 cluster due to their higher radial velocities. There is a suggestion that the Cen 45 spirals are at a larger distance than the Cen 45 ellipticals, but the 900 km s^{-1} difference is only two standard deviations. From dis-
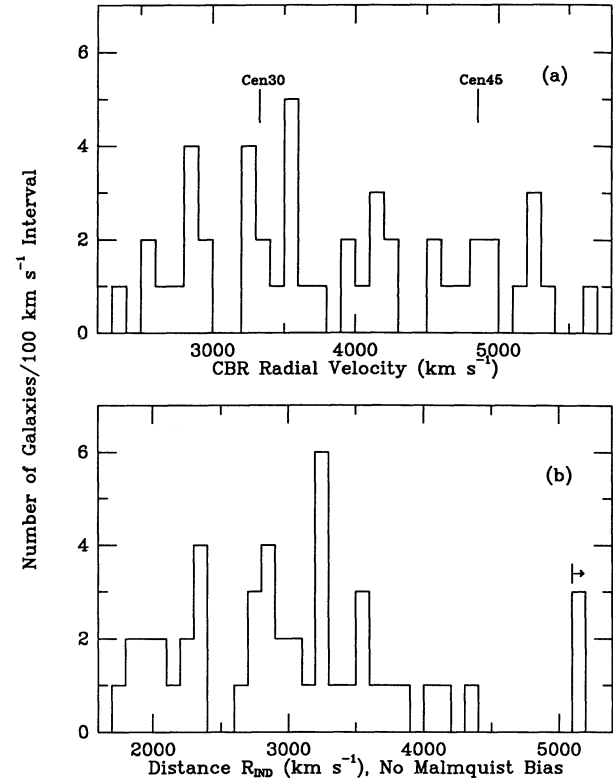

FIG. 6.—(a) The distribution of radial velocities (in the CBR reference frame) of the 47 Centaurus galaxies in 100 km s^{-1} intervals. (b) The distribution of distances for the same galaxies; the three galaxies with distances greater than 5100 km s^{-1} are lumped together. Nominal radial velocities of Cen 30 and Cen 45 from Lucey, Currie, and Dickens (1986) are marked in (a). Note the absence of a double peak in the radial velocity distribution, and the large range of distances in (b).

tance measurements alone, we therefore have little evidence for two separate clusters. In addition, the radial velocities of the 47 galaxies in Figure 6a show little evidence of the *bimodal* radial velocity distribution that is central to the inference that two clusters are situated along the line of sight. This lack of bimodality is not surprising, however, being similar to that found by Lucey et al. for the brighter galaxies in this region (their Fig. 4), from which the present measured galaxies were presumably chosen.

The current ambiguous situation could have probably been predicted from combining the initial Lucey et al. analysis and the 7S survey: As Lucey et al. stated, the galaxies in Cen 30 and Cen 45 are at about the same distance, or at least the same *range* in distance. There is a double-peaked character to the radial velocity distribution that could be due partly to the motion of two clusters relative to each other and partly to confusion with background galaxies at the higher redshift. Gravity induces a considerable dispersion in the radial velocities, which smears the structure even more.

If all 47 galaxies are treated as belonging to one cluster, the range in measured distance is somewhat larger than that seen for most other populous clusters (e.g., Coma and Virgo). It is not, however, larger than that seen for the other populous cluster located at low Galactic latitude, namely Perseus (Lynden-Bell et al. 1988). Although the *average* reddenings for the Centaurus and Perseus galaxies are not seriously in error (see Lynden-Bell et al. and the Appendix), the random errors in those reddenings could be larger, resulting in larger random
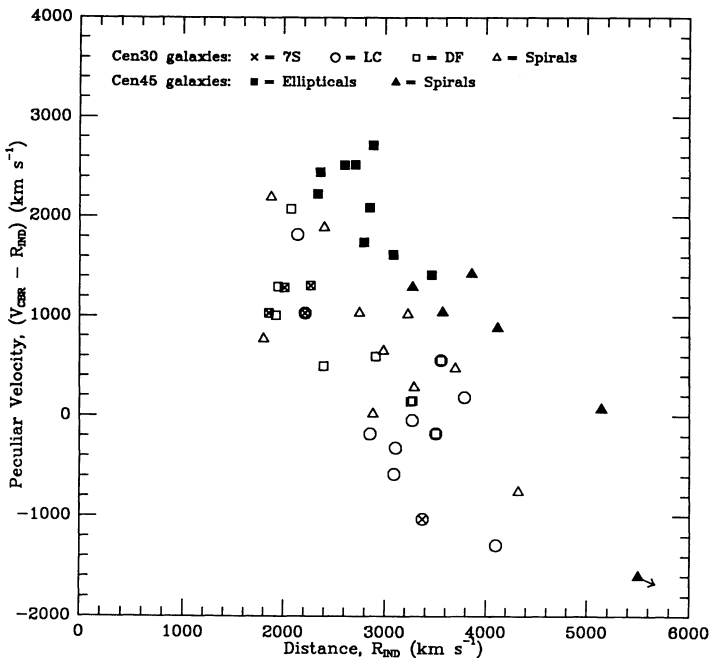

FIG. 5.—Peculiar velocity ($V_{CBR} - R_{IND}$) plotted against distance R_{IND} not corrected for Malmquist bias, for the 47 galaxies belonging to either Cen 30 or Cen 45. Individual radial velocities are used for this diagram. The elliptical galaxy data are averages of all observations by all observers. Data for Cen 30 E/S0 galaxies are plotted chronologically to show the growth in the data over the past several years: crosses represent the five galaxies observed by 7S; open circles represent 13 galaxies used by Lucey and Carter (1988); open squares represent 13 galaxies of the Dressler-Faber sample; 22 galaxies in all. Multiply measured galaxies have symbols overplotted. Cen 45 E/S0 galaxies are represented as closed squares. Spirals in Cen 30 are represented by open triangles; spirals in Cen 45 are represented as closed triangles (see legend). As noted by an arrow, one Cen 45 spiral is off the graph at coordinate (+7400, −2068).

errors in distance. Thus, the alternate view is to treat these clusters as if most galaxies are members of a single cluster with high internal velocity dispersion and distance errors, superposed on a background field of galaxies (the extended GA region) at ~ 4500 km s^{-1}.

Whether the system is viewed as comprised of one cluster or two infalling toward each other, the net peculiar motion of these 47 galaxies should be calculated as that of a single gravitationally bound unit. As such, we have calculated the distance of the combined Cen 30 + Cen 45 system in two ways in Table 2B: (1) as separate clusters (E/S0 galaxies only), with a net distance of the two calculated on the basis of a 3:1 ratio of mass of Cen 30:Cen 45 (from Lucey, Currie, and Dickens 1986), or (2) the median distance and radial velocity for all 47 galaxies treated as a single cluster (Table 2B). The peculiar motions of the Centaurus galaxies are plotted in Figure 2 both ways, and both methods imply a net *bulk* motion of these galaxies of ~ 750 km s^{-1}. Thus, viewed either way, the Centaurus galaxies are clearly in the *foreground* of the zero-crossing region at ~ 4500 km s^{-1}, and their gravity cannot be a major source of acceleration for the GA flow as a whole.

Finally, it is worth taking special note of the motions of spiral galaxies in the GA region, separate from the E/S0 galaxies. Within Centaurus, the spirals have motions generally consistent with the E/S0 galaxies (Fig. 5), except perhaps for galaxies assigned to Cen 45, where some of the spirals may truly be background. In addition to the Centaurus clusters, A89 and A86 measured motions for five other clusters in the GA region, all with low peculiar motions ranging from 100 to 600 km s^{-1}. However, these five clusters are at larger angular distances from the infall center, and their low motions are in fact consistent with the general infall picture (Fig. 3).

Besides the clusters, there are an additional 14 field spirals from A89 and Aaronson et al. (1982b) that are well placed on the near flank of the GA and within a 30° radius of the infall center. These galaxies were not considered by A89 in their analysis but are included here (open triangles and hexagons in Fig. 2 and Figs. 3a–3c). These show a large average motion of ~ 800 km s^{-1} and agree well with the model curves and the motions of other galaxies nearby. We conclude that the total published spiral data are, in fact, in good agreement with the general GA picture outlined by Lynden-Bell et al.

VI. INDEPENDENT CHECKS OF THE DISTANCE INDICATORS

The accuracy of the measured motions depends directly on the reliability of the distance estimators. Possible criticisms fall into two categories: (1) Galactic absorption errors and (2) variations in the zero points of the distance-indicator relations. In the Appendix, we explicitly test both possibilities. The quantity $\log_{10}(V/R)$ ($V = V_{CBR}$) is a measure of the peculiar velocity measured for each object. For the 7S galaxies, $\log_{10}(V/R)$ is compared to Galactic absorption, measures of cluster richness, stellar population, and galaxy absolute luminosity. No correlation is found with cluster richness or Galactic absorption. Possible weak correlations are found with stellar population for the single galaxies and intrinsic luminosity for cluster galaxies, but the observed effects are marginal and affect few galaxies. Most important, there is no evidence that the zero points are varying systematically with environment or direction on the sky. In particular, we find no evidence to support the claims of environmental effects put forward by Djorgovski, De Carvalho, and Han (1989). Similar tests of the spiral galaxies (Burstein 1990c, in preparation) yield null or negligible results.

In addition to these quantitative tests, there are several other strong arguments to support the distance indicators:

1. *Agreement among different distance indicators.*—Gunn (1989) has noted that the D_n-σ and Tully-Fisher relations are really two quite different physical relations. D_n-σ is simply a restatement of the virial theorem for ellipticals, coupled with the assumption of well-behaved (i.e., smoothly varying) M/L (Faber et al. 1987). The Tully-Fisher relation in contrast is much more demanding. Unlike D_n-σ, it involves only two parameters rather than three, and to eliminate the third parameter requires an additional constraint, which is probably imposed at galaxy formation. Thus, the TF relation tells us about galaxy *formation*, while D_n-σ tells us mainly about galaxy *equilibrium*. M/L regularity does enter both relations, but the stellar populations in the two galaxy types are quite different with regard to mean age and probably even mode of star formation. It would be a remarkable fact if M/L variations in both types of galaxies were the same.

Yet a third distance indicator has recently been proposed by Donnelly et al. (1989). This method relates X-ray luminosity to optical luminosity for early-type galaxies. A plot of these two quantities shows reduced scatter when D_n-σ distances are used in place of standard Virgo flow–corrected radial velocities. From the residuals of cluster galaxies, it appears that the errors in this method are uncorrelated with errors in D_n-σ. Hence the test is an independent verification of the D_n-σ method.

2. *Agreement between the observed motions and known concentrations of galaxies.*—The velocity field derived from measured galaxy motions is quite consistent with the gravitational accelerations expected from nearby galaxies. Much of the work that will quantitatively demonstrate this fact is now in progress (Dekel, Bertschinger, and Faber 1990, in preparation), but the basic picture is already clear. Other than the great attractor, features that are predicted and seen include the contraction of the Virgo–Ursa Major complex (Burstein 1990a, b), the motion of the Local Group and its environs toward the more populated side of the supergalactic plane, and a saddle point in the GA flow toward Perseus-Pisces, which divides that region from the region dominated by the great attractor.

Equally noteworthy is the discovery, completely after the fact, of the GA core in optical catalog data. Previously unknown, this major mass concentration was predicted *solely* on the basis of the observed velocity flow pattern. When searched, the ESO Catalog revealed a striking concentration of galaxies in the right direction (Lahav, as quoted by Lynden-Bell et al.), and the subsequent radial velocity survey by Dressler (1988) placed it at the right velocity. Moreover, the total observed mass excess is consistent with the overdensity required by the spherical flow model (Dressler 1988).

3. *Agreement among galaxies of different Hubble types in different environments.*—As shown in Figures 2 and 3, motions of spirals and ellipticals agree, and field galaxies agree with cluster galaxies. This agreement is true over the whole sky, not in just the GA region (Faber and Burstein 1989).

Thus there can be no doubt that, at some level, the measured flow velocities contain a strong grain of truth. The one remaining question, it seems, is the magnitude of the coherent, *bulk* flow over the region from the center of the GA on one side, to a distance of 1500–2000 km s^{-1} on the opposite side of the Local Group (see Faber and Burstein 1989; Burstein 1990b). The high value and degree of coherent motion in this volume seem to be discrepant with both hot and cold dark matter universes (Bardeen et al. 1986; Bertschinger and Juszkiewicz 1988;

Groth, Juszkiewicz, and Ostriker 1989; Gorski *et al.* 1989; but see Kaiser and Lahav 1989 for a dissenting view). They are also at variance with the bulk flow velocity originally predicted from the *IRAS* galaxy counts (as reported by Strauss and Davis 1989 and Yahil 1989).

Both these problems could be alleviated simply by adding a constant vector to "correct" (i.e., reduce) the measured galaxy velocities. To achieve agreement, this vector would have to have an amplitude of 300–400 km s^{-1} in a direction roughly *antiparallel* to the direction of the GA (i.e., toward $l \cong 130°$, $b \cong -20°$). However, the addition of such a vector would be equivalent to changing the adopted local standard of rest. Since our chosen standard of rest is the cosmic background radiation, we offer arguments in defense of that choice in the next section.

VII. THE COSMIC BACKGROUND RADIATION AS THE PREFERRED LOCAL STANDARD OF REST

The arguments in favor of the CBR as *the* standard of rest are perhaps not yet conclusive, but they are weighty:

1. Abandoning the CBR requires the ad hoc addition of a nonvelocity $\Delta T/T$ dipole term to the CBR intensity over the sky. This addition must be achieved without at the same time introducing any measurable multipole terms of higher order. The ratio of the higher order terms to the dipole term must be $\lesssim 10^{-5}/10^{-3}$, or $\leq 1\%$. Such a high ratio is not expected in current theories for the generation of structure in the universe. Achieving this goal could require very special initial conditions in the early universe, or alternatively, a very special location for the Local Group.

2. It is remarkable that the amplitude of the required dipole term is just comparable to the size of *real* gravity-induced motions in the universe (e.g., infall into the Local Supercluster).

3. It is still more remarkable that the direction of the $\Delta T/T$ dipole should point, just by chance, in precisely the right direction to produce a "spurious" great attractor. In other words, the vector turns out to point, with a high degree of precision, toward the largest, nearest, and most significant overdensity of galaxies in the neighborhood of the Local Group. To get the model to work requires alignment to within roughly 30° on the sky, which has a probability of chance occurrence of only 7%.

4. Three independent pieces of evidence appear to show a *return to the CBR standard of rest on large scales*: (*a*) the turn-over in peculiar motion beyond ~ 2000 km s^{-1} toward the GA (this paper; Dressler and Faber 1990), (*b*) the decline in bulk flow velocity in the 7S data away from the GA (Lynden-Bell *et al.* 1988; Faber and Burstein 1989), and (*c*) the small bulk motion of distant spiral-rich clusters in directions away from the GA (A86). The point is perhaps not yet conclusive, because the formal errors of all three measurements are individually large enough to admit a zero-point shift of 300–400 km s^{-1}. Taken together, the three studies are highly suggestive.

As stated in our first paper on this subject (Burstein *et al.* 1986), the collective weight of these arguments is such that we view abandoning the CBR as the standard of rest much like opening Pandora's box: it generates far more questions than it answers.

VIII. SUMMARY

We have combined all available data to produce a unified view of galaxy motions toward the great attractor. We have grouped ellipticals and spirals into clusters to reduce Malm-

quist bias and have utilized field spiral galaxies not previously analyzed. The current data base for galaxies within 40° of the GA has been expanded by a factor of 3.5 over the 69 galaxies in the original 7S survey.

The major conclusions are as follows:

1. All data sets agree with one another and support the basic picture of the flow in Lynden-Bell *et al.* (1988), as revised by Faber and Burstein (1989). Velocities rise outward from the Local Group toward the GA center to approximately 2000 km s^{-1} and decline beyond that point to zero (or near zero) at ~ 4500 km s^{-1}. The existence of a turnover, inferred by Faber and Burstein from only seven independent galaxies and groups, is now strongly confirmed.

2. The zero crossing point at ~ 4500 km s^{-1} is close to the centroid of the radial velocity peak identified by Dressler. This region can therefore plausibly be equated with the center of mass of the GA.

3. Peculiar motions derived from ellipticals and spirals, field and cluster galaxies all agree well, giving additional credence to the reality of the observed distances and motions.

4. The galaxies within the Centaurus region can alternately be viewed as populating two closely interacting clusters (e.g., Cen 30 and Cen 45 as defined by Lucey, Currie, and Dickens 1986), or as a single cluster having both a wide velocity dispersion and some range of measured distances along the line of sight. In either case, the Centaurus galaxies are located on the near side of the GA center and have a net peculiar motion of ~ 750 km s^{-1}, consistent with the overall GA flow. Thus, the present data are not consistent with the idea that the Centaurus clusters themselves are the gravitational source of the global infall.

5. A falloff in flow velocity is detected with angular distance away from the GA. This falloff is approximately symmetric about the center of the GA and, as such, it is reasonably matched by the simple spherical inflow model. The spherical model has been found to be a useful description of the motions over the volume so far surveyed (Burstein 1990*b*).

6. The observed peculiar motions are compared to Galactic absorption, cluster richness, stellar population, and absolute luminosity parameters of the elliptical galaxies. A marginal effect of stellar population differences on the predicted distances for field galaxies might exist, but few galaxies are involved, and these galaxies are distributed randomly on the sky. Low-luminosity ellipticals in clusters also show systematic deviations, but this does not affect the median cluster distances, nor the field galaxies, which are brighter. The net result is that we find no evidence that systematic errors can either produce, or seriously affect, the large-scale motions that are seen.

7. Despite efforts by DF to compile a deeper sample, the backside regions of the GA are still not yet clearly delineated. Because of Malmquist bias and sampling vagaries, we do not yet have an unambiguous profile of either the space density or the infall velocity through and beyond the GS. This lack will hopefully be remedied by a new spiral survey by the same authors, now underway.

APPENDIX

TESTS OF THE ELLIPTICAL DISTANCE INDICATORS VERSUS GALACTIC ABSORPTION, ENVIRONMENT, AND GALAXY STRUCTURE

I. GALACTIC ABSORPTION

The estimated center of the great attractor is located at low Galactic latitude ($\sim 18°$) in a region that is seriously affected by Galactic absorption (see Fig. 1). With the D_n-σ method, a change in the adopted absorption affects the measured distance in the following way:

$$\delta \log_{10} (R) = -0.32 \delta A_B,$$

where δA_B is the absorption measured in magnitudes. Thus, an increase in adopted absorption by 0.10 mag decreases distance by 7.4%.

With the exception of one region, the absorption estimates for all E/S0 galaxies here are taken directly from Burstein and Heiles (1982). The exception is the region bounded by $l = 230°$–$310°$, $b = -20°$ to $20°$, which Lynden-Bell et al. discovered had a high gas-to-dust ratio using the $(B-V)$-Mg_2 relation. Galaxies in this region showed colors that were systematically too blue when corrected by Burstein-Heiles reddenings (which in this region are based only on neutral hydrogen column densities). Lynden-Bell et al. estimated the extinctions to these galaxies directly from the $(B-V)$-Mg_2 relation. We cannot use that method here for the new E/S0 galaxies, since $(B-V)$ colors are not available for most of these galaxies. Instead, based on the corrections applied to the original 7S data, we have assumed a mean correction factor of 0.5 for the new extinctions in the anomalous area. A correction of this size in a specific region is no surprise, because similar gas-to-dust ratio variations are seen where galaxy counts are available (Burstein and Heiles 1982).

A test of whether residual absorption errors are distorting the derived motions is shown in Figure 7, which plots $\log_{10} (V/R)$ (defined in § VI) versus A_B for the E/S0 galaxies and clusters in the GA region, as noted in the figure caption. An arrow is plotted in Figure 7, showing the error line for $\delta A_B = \pm 0.10$ mag. This is comparable to the maximum allowed error for the 7S galaxies, most of which have extinctions predicted from the $(B-V)$-Mg_2 relation.

Four points are evident: first, there does appear to be a general trend for galaxies with higher absorption to show higher motions (both positive and negative). However, this is probably due more to the location of the GA center at low Galactic latitude than to errors in reddening: the most rapidly moving galaxies also should be among the most heavily reddened. Second, the double-ended arrow shows the sense of reddening errors. The slope is such that it might be possible to blame the motions of a few galaxies on reddening errors, but fully half the galaxies do not agree. Third, the galaxies in the anomalous region just described do not have peculiar motions that are significantly different from those of the galaxies outside this region. Many of these galaxies are far from the GA center and thus should have relatively small motions, as they do. Fourth, the motions of the new DF galaxies do not differ
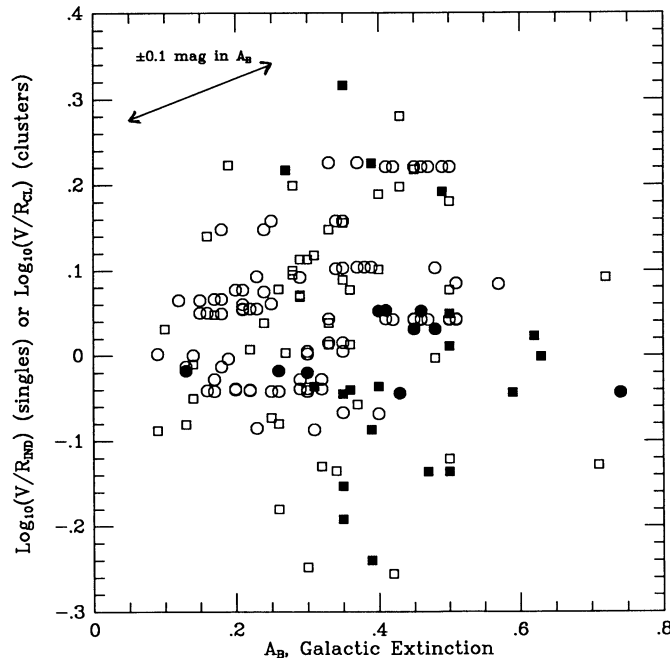

FIG. 7.—The logarithm of the ratio of predicted distance (Malmquist bias–corrected) to CBR radial velocity, $\log_{10} (V/R)$ plotted vs. galactic extinction A_B for galaxies in two regions near or around the GA. Open symbols are in the region $250° < l < 350°$, $40° < b < -40°$, except galaxies which lie in the region $230° < l < 310°$, $-20° < b < 20°$ are represented by closed symbols. Circles (closed and open) are galaxies in clusters; squares (closed and open) are field and single galaxies. R_{IND} is used for singly observed galaxies, R_{CL} for cluster galaxies. A double-ended arrow representing the effect of an extinction error of ± 0.10 mag in A_B is shown. The region that is singled out is one in which a high gas-to-dust ratio was found by Burstein et al. (1987), causing revisions in the extinction prediction.

statistically from those of the 7S galaxies in the anomalous region, indicating that our correction to the Burstein-Heiles extinctions in this region is reasonable.

We conclude that Figure 7 shows no evidence of significant systematic distance errors due to systematic errors in absorption estimates. Similar tests have also been carried out for the spiral galaxies, using both the extinctions used in those papers (based on the extinction method of the *Second Reference Catalog of Bright Galaxies* (de Vaucouleurs, de Vaucouleurs, and Corwin 1976) and on Burstein and Heiles values. Again, no systematic trends of peculiar motions with either set of extinctions are seen.

These results buttress our earlier argument in § III against errors in absorption artificially producing the observed motions. It was noted there that a constant absorption error in magnitudes produces an error in peculiar motion that is proportional to distance. Absorption errors cannot cause the global pattern and turndown seen in velocity in Figures 2 and 3 unless they are (miraculously) correlated with distance and position on the sky. Figure 7 supports this point explicitly by showing that there is no global trend between absorption and peculiar motions in this region of the sky.

II. ZERO-POINT VARIATIONS WITH ENVIRONMENT

A second possibility (Djorgovski, De Carvalho, and Han 1989, hereafter DDH; Silk 1989) is that the zero points of the D_n-σ and Tully-Fisher relations vary throughout space in such a way as to mimic, by chance, a great attractor flow. In particular, DDH have claimed to find a correlation between D_n-σ slope (and slope variations) with cluster richness. If true, this would raise the possibility that *zero point* is also a function of environment.

We can further test this claim in three ways. First, the sources used for cluster richness are not given by DDH, and we find that the richnesses used in their graphs are not supported by any published data (the six clusters used in their paper can be readily identified by comparing with the table of slopes in Appendix B of Lynden-Bell *et al.* 1988). DDH richnesses are compared to various values taken from the literature in Table 3. We provide two measures of richness, central density (Bahcall 1977) and total richness. In addition, we add two 7S clusters not considered by DDH. There is clearly no correlation between either richness measure and the rankings assigned by DDH. This latter point is emphasized by the fact that the Virgo, Coma, and Fornax Clusters all have similar D_n-σ slopes but span the full known range in cluster richness.

DDH have also measured a slope difference in the D_n-σ relation between the inner and outer galaxies in a cluster and claim that this is correlated with cluster richness. However, the data become very noisy when broken up in this way. Several of the inner slopes determined by DDM are manifestly ridiculous—one is even negative! The claimed slope differences are simply based on too few galaxies.

Third, it is not sufficient merely to isolate a possible slope dependence with environment; one must also demonstrate that environmental effects translate directly into a net dependence of *peculiar motion* on environment. The peculiar motions of clusters are based on the median distance as determined from many galaxies, and slope errors would cancel in the final value. This additional step was not taken by DDH. We take it here using total group richnesses as tabulated by Geller and Huchra (1983) and Huchra and Geller (1982) for the 7S elliptical groups. The tabulated group populations have been corrected for redshift and reddening using the measured distances and a standard Schechter (1977) luminosity function (for details, see Table 3). To these we

TABLE 3
D_n-σ SLOPE VERSUS CLUSTER RICHNESS AND CLUSTER DENSITY

Cluster	Slope	DDH Richness[a]	Bahcall Richness[b] (density)	Total Richness[c]
Fornax	1.16 ± 0.27	-1	13	61
Perseus	1.56 ± 0.28	0	33	1006
Coma	1.24 ± 0.11	1	28	1184
Virgo	1.37 ± 0.12	1	11	257
Abell 2199	0.88 ± 0.41	2	19	1006
DC 2345−28	0.88 ± 0.36	3	14	373
Eridanus	1.02 ± 0.29	...	low	101
Abell 194	0.83 ± 0.25	...	...	138

[a] Richness assigned by Djorgovski, De Carvalho and Han 1989.

[b] Bahcall richness (Bahcall 1977): this is the number of galaxies within 2 mag of the third brightest galaxy within a diameter of 1 Mpc ($H_0 = 50$). Values for Perseus, Coma, Abell 2199, DC 2345−28, and Virgo are taken directly from Bahcall. Fornax has been scaled to Virgo by counting in the *Nearby Galaxies Atlas* (Tully 1988). Bahcall richness is more a measure of central density then total richness.

[c] Total richness: this is the total number of galaxies down to $M_B = -17.0$, corrected for absorption and assuming $H_0 = 50$. The basis of the scale is the corrected richnesses of the Huchra and Geller (1983) and Geller and Huchra (1983) groups. These can be computed directly from the data given in these papers for Coma, Virgo, Eridanus, Fornax, and Abell 194 (for Virgo, we include only galaxies north of decl. $= 7°$). Perseus and Abell 2199 have been scaled to Coma using Abell counts quoted by Bahcall (1977). DC 2345−28 has been taken from Dressler (1980) with corrections for total area and magnitude limit (similar corrections for other Dressler clusters matched Huchra and Geller and Geller and Huchra to within $\pm 25°$).

add richnesses for large clusters on the same scale from Table 3. Field galaxies from 7S and DF (not assigned to any group) round out the sample, with assigned richness = 1.

These richness data [calculated as log (number of galaxies brighter than $M_B = -17$)] are compared to $\log_{10} (V/R)$ in Figure 8, with R_{IND} used for field and single and R_{CL} used for clusters. No trend is evident over nearly a range of 1000 in richness. We conclude that environment as measured by group richness has no effect on the slope or zero point of D_n-σ.

We have not made the same plot with spiral data because the membership of spiral groups is more problematical. However, based on the nominal, published memberships, one can foresee immediately that there will be no trend here either. This is because the spiral motions agree well with the E galaxies, and the plot will therefore simply duplicate Figure 8.

To summarize, there is no evidence that the slopes or zero points of the distance relations are modulated by environment in any significant way.

III. ZERO-POINT VARIATIONS VERSUS OTHER GALAXY PARAMETERS

For the 7S ellipticals, there are additional parameters that can be used to test for zero-point variations. These include Mg_2, ΔMg_2 (relative to $\log \sigma$), $(B-V)_0$, $\Delta(B-V)_0$ (relative to Mg_2), envelope type, effective radius, surface brightness, and absolute luminosity (see Faber et al. 1989). Of these, $\Delta(B-V)_0$, ΔMg_2, and absolute luminosity are the most interesting because they might signal differences in stellar populations and hence in M/L.

Burstein et al. (1988) have shown that Mg_2 and $(B-V)_0$ are closely correlated for the 7S sample, with scatter compatible with observational errors. Moreover, it is shown there that Mg_2 and $\log \sigma$ are also correlated, but with some intrinsic scatter toward weaker values of Mg_2.

Plots of ΔMg_2, $\Delta(B-V)_0$, and absolute luminosity, M_B, versus $\log_{10} (V/R_{IND})$ are shown in Figures 9a–9e for field and single E/S0 galaxies and E/S0 galaxies in clusters with four or more measured galaxies (here R_{IND} is used for cluster galaxies, as we wish to explore the residuals of individual galaxies). There is no correlation in Figures 9a and 9b, which indicates once more that extinction does not systematically affect the data.

In Figures 9c and 9d, ΔMg_2 is tested versus $\log_{10} (V/R_{IND})$, and here the results are a little ambiguous. Singly observed galaxies appear to have values of ΔMg_2 that become smaller with lower predicted distances. The effect is weak, but it is in the sense of the effect that star formation would have on both D_n and Mg_2: increasing star formation increases the brightness of a galaxy, thereby increasing the size of D_n, placing the galaxy apparently closer. Star formation would also dilute the observed strength of Mg_2, while probably leaving $\log \sigma$ unaffected.

However, the amount of star formation required to change a distance by 0.2 dex would have to change the apparent magnitude by 0.65 mag (from the dependence of D_n on changes in magnitude, given in § I of this Appendix), which in turn would produce a very large change in Mg_2 (~0.15 mag). Such a large change in Mg_2 is not observed. In addition, the spread in ΔMg_2 is the same for both cluster and singly observed galaxies, and a similar effect is not seen for the cluster galaxies (Fig. 9d). Since the number of singly observed galaxies affected is small (less than 20) and randomly distributed on the sky, this scatter is simply contributing to noise in the measured motions.

A test of the dependence of $\log_{10} (V/R_{IND})$ with absolute luminosity can only be done for cluster galaxies, because the necessary
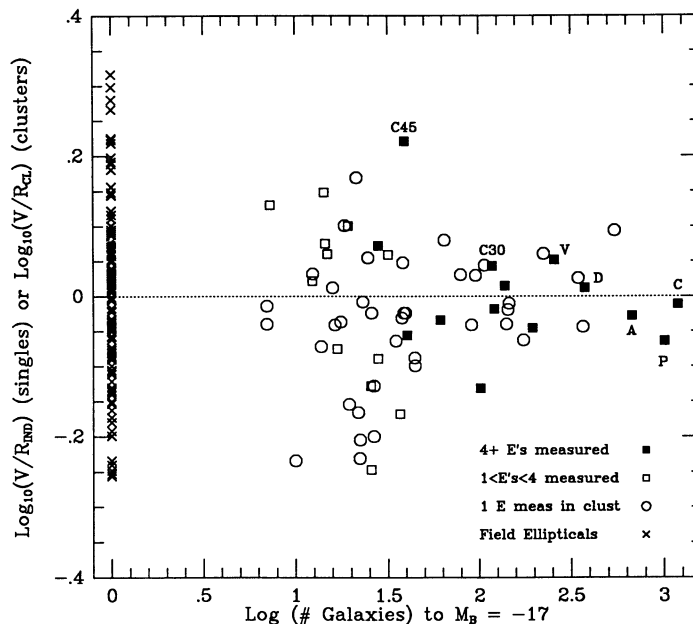

FIG. 8.—$\log_{10} (V/R)$ plotted vs. the logarithm of the estimated number of galaxies in a cluster with absolute magnitude M_B brighter than -17, for elliptical galaxy distances with median distances for different numbers of cluster members, as given in the legend. Field galaxies are included with richness defined as 1. A few well-known clusters are noted: C45 = Cen 45; C30 = Cen 30; V = Virgo; A = Abell 1367; P = Perseus; C = Coma. No trend of peculiar motion with cluster richness is seen. R_{IND} is used for "singles" and field galaxies, R_{CL} for clusters.
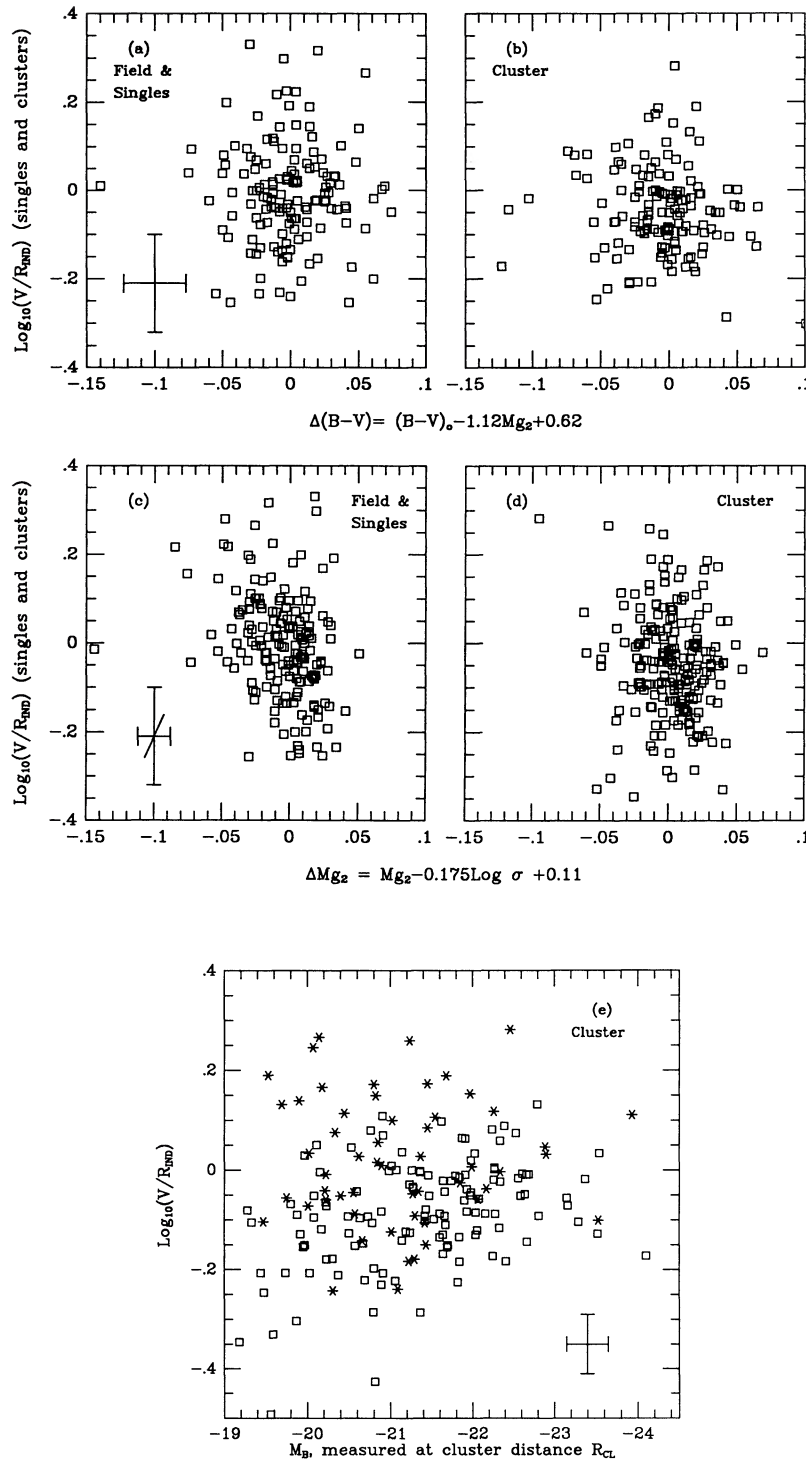
Fig. 9.—Three tests of possible systematic errors in the distance estimates, using E/S0 field and "singles" and E/S0 galaxies in clusters with four or more measured galaxies. $\log_{10}(V/R_{\rm IND})$ is used for all galaxies. (a) and (b) $\log_{10}(V/R_{\rm IND})$ plotted vs. the residual of $(B-V)_0$ color with respect to the Mg_2 line index, assuming the relation $(B-V)_0 = 1.12\,Mg_2 + 0.62$ for 140 field/single E/S0 galaxies in (a) and 138 cluster E/S0 galaxies in (b). No correlation is seen, indicating reddening errors are not systematically affecting distance estimates. (c) and (d) $\log_{10}(V/R_{\rm IND})$ plotted vs. the residual of Mg_2 line strength with central velocity dispersion, σ, assuming the relationship $Mg_2 = 0.175\log\sigma - 0.11$, for 171 singly observed E/S0 galaxies in (c) and 211 cluster E/S0 galaxies in (d). Errors in the two coordinates are correlated as shown, since $\log\sigma$ enters into each parameter. The weak possible dependence of predicted distances on stellar population indicated by the singly observed galaxies is not confirmed by the cluster galaxies. (e) $\log_{10}(V/R_{\rm IND})$ plotted vs. absolute B magnitude for 182 E/S0 galaxies in clusters. Errors in the two coordinates are relatively uncoupled, because median distances of clusters are used to calculate M_B. Open squares are galaxies measured only by 7S; six-sided stars are galaxies measured by DF.

use of distance in the calculation of both parameters leads to strongly correlated errors for singly observed galaxies. To avoid such problems, only galaxies from clusters that have at least four galaxies with measured distances are used, and their absolute magnitudes are calculated based on the cluster distance, R_{CL}. Since M_B values are available only for DF and 7S galaxies, the galaxies from the two samples are individually identified in Figure 9e.

As noted by Bertschinger (private communication), a weak correlation of $\log_{10} (V/R_{IND})$ with M_B is seen for the 7S data, perhaps increasing for galaxies fainter than $M_B = -20$. No such effect is seen for DF galaxies, causing one to suspect that the observed effect may be an artifact of the problems in determining total magnitudes for galaxies (see Burstein et al. 1987). [Please note that the larger values of $\log_{10} (V/R_{IND})$ for the DF galaxies simply reflects the fact that these galaxies have predominantly outward motions.] These intrinsically faint galaxies are not present in the field E/S0 data, a byproduct of Malmquist bias. The use of the median distances for clusters virtually eliminates whatever small systematic error that may result from this cause.

Finally, tests have also been made to see if envelope type correlates with peculiar motion; no trend is seen.

REFERENCES

Aaronson, M., Bothun, G. D., Mould, J. R., Huchra, J., Schommer, R., and Cornell, M. 1986, Ap. J., 302, 536 (A86).
Aaronson, M., et al. 1989, Ap. J., 338, 654 (A89).
Aaronson, M., Huchra, J., Mould, J., Schechter, P. L., and Tully, R. B. 1982a, Ap. J., 258, 64.
Aaronson, M., et al. 1982b, Ap. J. Suppl., 50, 241.
Bahcall, N. A. 1977, Ap. J. (Letters), 217, L77.
Bardeen, J. M., Bond, J. R., Kaiser, N., and Szalay, A. S. 1986, Ap. J., 304, 15.
Bertschinger, E., and Juszkiewicz, R. 1988, Ap. J. (Letters), 334, L59.
Burstein, D. 1990a, in Large-Scale Structures and Peculiar Motions in the Universe, ed. D. Latham and L. N. Da Costa, in press.
———. 1990b, Rept. Progr. Phys., in press.
———. 1990c, in preparation.
Burstein, D., Davies, R. L., Dressler, A., Faber, S. M., Lynden-Bell, D., Terlevich, R. J., and Wegner, G. 1986, in Galaxy Distances and Deviations from Universal Expansion, ed. B. F. Madore and R. B. Tully (Boston: Reidel), p. 123.
———. 1988, in Towards Understanding Galaxies at High Redshift, ed. R. G. Kron and A. Renzini (Dordrecht: Kluwer), p. 17.
Burstein, D., Davies, R. L., Dressler, A., Faber, S. M., Stone, R. P. S., Lynden-Bell, D., Terlevich, R. J., and Wegner, G. 1987, Ap. J. Suppl., 64, 601.
Burstein, D., and Heiles, C. 1978, Ap. J., 225, 40.
———. 1982, A.J., 87, 1165.
Burstein, D., and Raychaudhury, S. 1989, Ap. J., 343, 18.
Chincarini, G., and Rood, H. J. 1979, Ap. J., 230, 648.
Davies, R. L., Burstein, D., Dressler, A., Faber, S. M., Lynden-Bell, D., Terlevich, R. J., and Wegner, G. 1987, Ap. J. Suppl., 64, 581.
de Vaucouleurs, G., de Vaucouleurs, A., and Corwin, H. G. 1976, Second Reference Catalog of Bright Galaxies (Austin: University of Texas Press).
de Vaucouleurs, G., and Peters, W. L. 1984, Ap. J., 287, 1.
Djorgovski, S., De Carvalho, R., and Han, M.-S. 1989, in The Extragalactic Distance Scale, ed. S. van den Bergh and C. J. Pritchet (Provo: ASP), p. 329.
Donnelly, R., Hanks, Faber, S. M., and O'Connell, R. M. 1989, Ap. J., submitted.
Dressler, A. 1980, Ap. J., 236, 351.
———. 1988, Ap. J., 329, 519.
Dressler, A., and Faber, S. M. 1990, Ap. J., 354, 13 (DF).
Dressler, A., Faber, S. M., Burstein, D., Davies, R. L., Lynden-Bell, D., Terlevich, R. J., and Wegner, G. 1987, Ap. J. (Letters), 313, L37.
Faber, S. M., and Burstein, D. 1989, in Large-Scale Motions in the Universe, ed. V. C. Rubin and G. V. Coyne (Princeton: Princeton University Press), p. 116.

Faber, S. M., Dressler, A., Davies, R. L., Burstein, D., Lynden-Bell, D., Terlevich, R. J., and Wegner, G. 1987, in Nearly Normal Galaxies: From the Planck Time to the Present, ed. S. M. Faber (Boston: Springer-Verlag), p. 175.
Faber, S. M., Wegner, G., Burstein, D., Davies, R. L., Dressler, A., Lynden-Bell, D., and Terlevich, R. J. 1989, Ap. J. Suppl., 69, 763.
Fairall, A. P., and Winkler, H. 1984, in Clusters and Groups of Galaxies, ed. F. Mardirossian, G. Giuricin, and M. Mezzetti (Dordrecht: Reidel), p. 23.
Geller, M., and Huchra, J. 1983, Ap. J. Suppl., 52, 61.
Gorski, K., Davis, M., Strauss, M. A., White, S. D. M., and Yahil, A. 1989, Ap. J., 344, 1.
Groth, E. J., Juszkiewicz, R., and Ostriker, J. P. 1989, Ap. J., 346, 558.
Gunn, J. E. 1989, in The Extragalactic Distance Scale, ed. S. van den Bergh and C. J. Pritchet (Provo: ASP), p. 344.
Hopp, U., and Materne, J. 1985, Astr. Ap. Suppl., 61, 93.
Huchra, J., and Geller, M. 1983, Ap. J., 257, 423.
Kaiser, N., and Lahav, O. 1989, in Large-Scale Motions in the Universe, ed. V. C. Rubin and G. V. Coyne (Princeton: Princeton University Press), p. 339.
Kraan-Korteweg, R. C., Cameron, L. M., and Tammann, G. A. 1988, Ap. J., 331, 620.
Lucey, J. R., and Carter, D. 1988, M.N.R.A.S., 235, 1177 (LC).
Lucey, J. R., Currie, M., and Dickens, R. J. 1986, M.N.R.A.S., 221, 453.
Lucey, J. R., Lahav, O., Lynden-Bell, D., Terlevich, R. J., and Melnick, J. 1990, in Large-Scale Structures and Peculiar Motions in the Universe, ed. D. Latham and L. N. Da Costa, in press.
Lynden-Bell, D., Faber, S. M., Burstein, D., Davies, R. L., Dressler, A., Terlevich, R. J., and Wegner, G. 1988, Ap. J., 326, 19 (7S).
Melnick, J., and Moles, M. 1987, Rev. Mexicana Astr. Af., 14, 72.
Scaramella, R., Balesi-Pillastrini, G., Chincarini, G., Vettolani, G., and Zamorani, G. 1989, Nature, 338, 562.
Schechter, P. L. 1977, A.J., 82, 569.
Silk, J. 1989, Ap. J. (Letters), 345, L1.
Strauss, M. A., and Davis, M. 1989, in Large-Scale Motions in the Universe, ed. V. C. Rubin and G. V. Coyne (Princeton: Princeton University Press), p. 256.
Tully, R. B. 1988, Nearby Galaxies Atlas (Cambridge: Cambridge University Press).
Yahil, A. 1989, in Large-Scale Motions in the Universe, ed. V. C. Rubin and G. V. Coyne (Princeton: Princeton University Press), p. 219.

DAVID BURSTEIN: Department of Physics and Astronomy, Arizona State University, Tempe, AZ   85287-1504

ALAN DRESSLER: The Observatories of the Carnegie Institution of Washington, 813 Santa Barbara Street, Pasadena, CA   91101

S. M. FABER: Lick Observatory, University of California, Santa Cruz, CA   95064